Increased atherosclerosis in LDL receptor–null mice lacking ACAT1 in macrophages

Sergio Fazio,[1,2] Amy S. Major,[1] Larry L. Swift,[2] Linda A. Gleaves,[1]
Michel Accad,[3] MacRae F. Linton,[1,4] and Robert V. Farese, Jr.[3]

[1]Department of Medicine, Division of Cardiovascular Medicine, and
[2]Department of Pathology, Vanderbilt University Medical Center, Nashville, Tennessee, USA
[3]Gladstone Institute of Cardiovascular Disease, and Department of Medicine, University of California, San Francisco, California, USA
[4]Department of Pharmacology, Vanderbilt University Medical Center, Nashville, Tennessee

Address correspondence to: Sergio Fazio or MacRae F. Linton, Vanderbilt University Medical Center, Division of Cardiovascular Medicine, 315 Medical Research Building II, Nashville, Tennessee 37232-6300, USA. Phone: (615) 936-1450; Fax: (615) 936-1872; E-mail: sergio.fazio@mcmail.vanderbilt.edu or macrae.linton@mcmail.vanderbilt.edu.

During atherogenesis, circulating macrophages migrate into the subendothelial space, internalize cholesterol-rich lipoproteins, and become foam cells by progressively accumulating cholesterol esters. The inhibition of macrophage acyl coenzyme A:cholesterol acyltransferase (ACAT), which catalyzes the formation of cholesterol esters, has been proposed as a strategy to reduce foam cell formation and to treat atherosclerosis. We show here, however, that hypercholesterolemic LDL receptor–deficient ($LDLR^{-/-}$) mice reconstituted with ACAT1-deficient macrophages unexpectedly develop larger atherosclerotic lesions than control $LDLR^{-/-}$ mice. The ACAT1-deficient lesions have reduced macrophage immunostaining and more free cholesterol than control lesions. Our findings suggest that selective inhibition of ACAT1 in lesion macrophages in the setting of hyperlipidemia can lead to the accumulation of free cholesterol in the artery wall, and that this promotes, rather than inhibits, lesion development.

J. Clin. Invest. **107**:163–171 (2001).

Introduction

It is commonly believed that the accumulation of cholesterol esters in arterial macrophages is a deleterious process leading to the formation of foam cells. However, it is debatable whether the development of macrophages into cholesterol ester–rich foam cells promotes or inhibits atherosclerotic lesion development. On the one hand, the accumulation of cholesterol esters may trigger the development of lipid-rich lesions. Conversely, the accumulation of unesterified cholesterol in the absence of adequate efflux may have toxic effects (1). Cholesterol esters in macrophages and other cells are synthesized by acyl coenzyme A:cholesterol acyltransferase (ACAT), which uses free cholesterol and fatty acyl coenzyme A as substrates (2, 3). Many studies in animals have suggested that ACAT inhibitors reduce atherosclerotic lesion development by reducing intestinal cholesterol absorption, lowering plasma cholesterol levels, and by directly inhibiting macrophage foam cell formation in atherosclerotic lesions (4–6). Several inhibitors have been shown to reduce atherosclerosis in hypercholesterolemic animals at doses that did not lower plasma cholesterol levels (7–10), suggesting that direct inhibition of ACAT in macrophages may be a useful strategy in treating atherosclerosis (4).

Two mammalian ACAT genes have recently been cloned. ACAT1 (11–13), which is expressed highly in macrophages, adrenal glands, sebaceous glands, and steroidogenic tissues, is also expressed in atherosclerotic lesions (14, 15), where it serves as a major regulator of the cholesterol ester cycle in macrophages. ACAT2 (16–18) is expressed in the liver and intestine, where it plays a role in lipoprotein assembly (3). A recent report has indicated that the human liver expresses predominantly ACAT1, whereas human intestinal cells express mainly ACAT2 (19). Because most currently available ACAT inhibitors act nonselectively on both enzyme forms (16), it has not been possible to use inhibitors to test the hypothesis that the specific inhibition of ACAT1 in lesion macrophages would reduce atherosclerotic development. We attempted to examine this question in a previous study by crossing ACAT1-deficient mice (13) with atherosclerosis-susceptible strains such as apoE knockout mice (20) and LDL receptor–deficient ($LDLR^{-/-}$) mice (21). However, introducing systemic ACAT1 deficiency into these hyperlipidemic models resulted in extensive deposition of free cholesterol in the skin and brain (22). Accompanying this was a relative lowering of serum cholesterol levels in ACAT1-deficient mice, which precluded our ability to quantitatively assess lesions and determine the specific effect of ACAT1 deficiency on lesion size. Thus, it has remained unclear whether ACAT1 inhibition in macrophages would prevent atherosclerosis.

To address this question, we have now used a marrow transplantation model through which ACAT1-

deficient macrophages are introduced into LDL receptor–deficient mice, thereby avoiding the xanthomatosis caused by systemic ACAT1 deficiency. Unexpectedly, our results indicate that macrophage ACAT1 deficiency promotes, rather than inhibits, lesion formation.

Methods

Animal procedures. LDLR$^{-/-}$ mice backcrossed onto the C57BL/6 background were maintained in microisolator cages on a rodent chow diet containing 4.5% fat (catalog no. 5010; Purina Mills Inc., St. Louis, Missouri, USA) and autoclaved acidified (pH 2.8) water. The experimental protocols were performed according to the regulations of Vanderbilt University's Animal Care Committee.

Genetic background. The original ACAT1-null mice were created on a mixed background of C57BL/6 and 129/Sv (13). We backcrossed these mice for three generations with C57BL/6 mice before starting our first experiment using fetal liver cells. Although at that point the donor mice were only about 90% C57BL/6, the use of fetal liver cells eliminated the risk of graft-versus-host disease because these cells are immunologically naive and lack mature T cells (23). After the ACAT1-null mice reached the 10th backcross in the C57BL/6 background (>99.99% C57BL/6), we performed our second study using bone marrow transplantation. In all studies, the recipient mice were backcrossed in the C57BL/6 background for ten generations or more.

Diets. The western-type diet contains 0.15% cholesterol and no cholic acid, whereas the butterfat diet contains 1.25% cholesterol and 0.5% cholic acid. Both diets induce atherosclerosis in LDLR-null mice, but the degree of hyperlipidemia is higher with the butterfat diet. Given the unexpected and largely significant results of the first study, conducted using the western-type diet, we designed the second experiment with the intent of inserting variables that could potentially change the outcome of the intervention. For this reason, the second study was done using male LDLR-null recipients, LDLR$^{-/-}$ACAT1$^{-/-}$ donor marrow, and a more atherogenic diet.

Experimental design. In the first experiment, we used 14 mice in each of the three groups receiving donor fetal liver cells with the three possible ACAT1 genotypes. In the second experiment, we used six mice in each of the two groups receiving either ACAT1$^{+/+}$ or ACAT1$^{-/-}$ cells. A power calculation analysis based on data from the first experiment showed adequate power (0.99) to detect this effect again for a level of significance of $P < 0.05$ by using five mice in each group.

Fetal liver cell isolation. Female ACAT1$^{+/-}$ mice were mated with ACAT1$^{+/-}$ males, and pregnancy was determined by the presence of a vaginal plug. On day 14 of gestation, the mice were killed by cervical dislocation and the embryos were dissected from the placenta and yolk sac. The rest of the procedure was done as previously described (24).

Rapid PCR genotyping and sex identification. To identify the ACAT1 genotype of the fetuses, genomic DNA was amplified with the following primers: 5′-CAG CTA TGT ACA CAC ATA TAT TCA TG-3′, located upstream of the targeting vector; 5′-TTG GGA AGA CAA TAG CAG GCA TGC-3′, located in the polyadenylation signal of the Neo gene (the targeted allele yields a 833-bp band); and 5′-GGA CTT TTC AAT GAG GTT GGT CAC-3′, which is unique to the deleted region of the wild-type allele (and yields a 790-bp fragment) (13). The sex of the fetuses was identified using primers to detect the Zfy gene present in the sex-determined region of the Y chromosome (25).

Fetal liver cell transplantation. A week before, and 2 weeks after, transplantation, all recipient mice were given 100 mg/l neomycin and 10 mg/l polymyxin B sulfate (Sigma Chemical Co., St. Louis, Missouri, USA) in acidified water. Fetal liver cells were thawed rapidly at 37°C and washed in RPMI-1640 containing 2% FBS. Forty 12-week-old female recipient LDLR$^{-/-}$ mice were lethally irradiated (9 Gy) using a cesium gamma source, and 4 hours later, 5×10^6 cells in 300 μl of RPMI-1640 media were injected into the tail vein. After transplantation, the mice were placed on a rodent chow diet (catalog no. 5010.; PHI Feeds Inc., St. Louis, Missouri, USA) for 4 weeks and then on a high-fat western-type diet (21% fat and 0.15% cholesterol; Teklad Madison, Wisconsin, USA) for 12 weeks.

Bone marrow transplantation. This experiment was performed with male recipient LDLR$^{-/-}$ mice, and ACAT1$^{-/-}$ and LDLR$^{-/-}$ double-negative mice as donors. Additional differences from the described fetal liver cell transplantation studies included the use of bone marrow, rather than fetal cells, and the use of a more atherogenic diet. Bone marrow was collected from donor mice (LDLR$^{-/-}$ACAT1$^{+/+}$ or LDLR$^{-/-}$ACAT1$^{-/-}$) basically as described previously (26). Fifteen-week-old male recipient LDLR$^{-/-}$ mice were lethally irradiated 4 hours before transplantation with 9 Gy from a cesium gamma source. After transplantation, the mice were placed on a rodent chow diet for 4 weeks and then on a butterfat diet (ICN Biochemicals, Costa Mesa, California, USA) containing 19.5% fat, 1.25% cholesterol, and 0.5% cholic acid for 10 weeks.

Serum cholesterol and triglyceride analysis. Blood samples were collected by retro-orbital venous plexus puncture using heparinized tubes, and serum was separated by centrifugation and preserved using 1 mM PMSF (Sigma Chemical Co.). All blood collections were performed after a 4-hour fast. Serum cholesterol levels were determined using Sigma Kit no. 352 adapted for a microtiter plate assay (Sigma Chemical Co.) (27). Briefly, 100 μl of a 1:100 dilution of serum was mixed with 100 μl of reagent and incubated at 37°C for 10 minutes in a microplate reader (Molecular Devices Menlo Park, California, USA). Serum triglyceride levels were determined using Sigma Kit no. 339

similarly adapted for microtiter plate assay (Sigma Chemical Co.) (absorbency was read at 540 nm).

Quantitation of arterial lesions in cross sections at the aortic sinus. After 12 weeks on a western-type diet, the mice were sacrificed and flushed with 30 ml saline by slow injection through the left ventricle. The heart with aorta was embedded in OCT and snap-frozen in liquid nitrogen. Cryosections of 10-μm thickness were taken from the region of the proximal aorta starting from the end of the aortic sinus and for 300 μm distally, according to the procedure of Paigen et al. (28). Cryosections were stained with Oil-Red-O (Sigma Chemical Co.) and counterstained with hematoxylin. Quantitative analysis of lipid-stained lesions was performed using an Imaging System KS300 (Release 2.0, Kontron Elektronik GmbH). Color threshold was used to delimit the Oil-Red-O–stained lesion area that was measured as square microns per animal. Cryosections were counterstained with hematoxylin. This was done with the same procedure as in all our previous studies (26) with the exception that, due to the spotty staining with Oil-Red-O (a consequence of lack of ACAT1 and presence of large areas of acellular material), the manual overrule of the color threshold was done more often than usual. The operator was blinded to the group assignment of the sections analyzed.

Assessment of aortic atherosclerosis in en face preparations. The mice were flushed with 30 ml of saline by slow injection through the left ventricle. The entire aortae, from the aortic valve to the iliac bifurcation, were dissected out and cleaned of any adipose and connective tissue attached to the adventitia. After overnight fixation with 4% paraformaldehyde, the aortae were opened longitudinally with extremely fine Vanna microscissors (Fine Science Tools Inc., Foster City, California, USA) and pinned flat on a black surface in a dissecting pan with 0.2-mm-diameter stainless steel pins. The aortae were stained with Sudan IV and photographed (29). Comparisons of lesion area affected by atherosclerosis (as percent of total vascular surface) were done by computerized analysis, as described for the cross sections.

Quantitation of arterial cholesterol. Aortic cholesterol was analyzed essentially as described (30). The full aorta, from the arch to the iliac bifurcation, was removed and cut into small pieces, placed in chloroform/methanol (2:1 vol/vol) containing 5 α-cholestane as an internal standard, and homogenized. The homogenate was kept at 4°C for at least 1 hour, and then 2 volumes of ethyl ether were added and the protein was pelleted by centrifugation. The lipid extract was dried under nitrogen and dissolved in hexane. Unesterified cholesterol was analyzed in an aliquot of the extract by gas chromatography using a Hewlett-Packard 5890 gas chromatograph (Hewlett-Packard Co., Palo Alto, California, USA) equipped with a DB-17 column (0.53 mm internal diameter × 15 m × 1 μm film; J&W Scientific Inc., Folsom, California, USA) and flame ionization detector. The oven temperature was 250°C. To determine total cholesterol, a second aliquot of the extract was saponified with 0.4% ethanolic KOH. The non-saponifiable sterol was extracted using hexane, and total cholesterol was determined using the gas chromatograph. The difference between total cholesterol and free cholesterol is esterified cholesterol, and the mass of cholesterol ester is calculated as 1.67 × esterified cholesterol. The protein pellet was solubilized in 1N NaOH and protein was determined by the bicinchoninic acid assay (Pierce Chemical Co., Rockford, Illinois, USA) using BSA as standard.

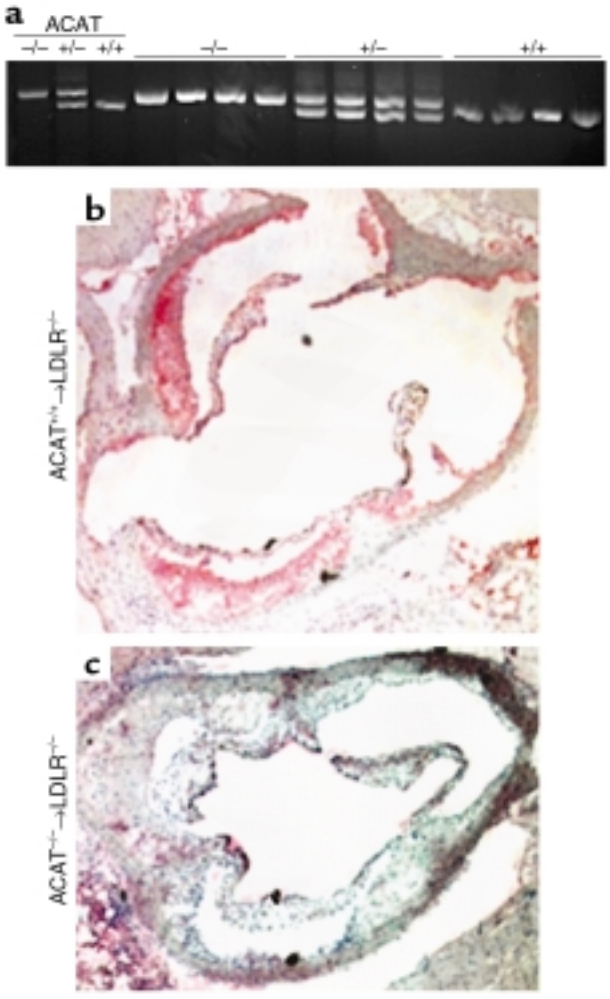

Figure 1
Reconstitution of recipient mice with donor marrow. (**a**) ACAT1 genotyping in recipients of fetal liver cell transplants. DNA was prepared from the bone marrow of LDLR$^{-/-}$ recipient mice at least 4 weeks after transplantation. The genomic DNA was amplified in a PCR reaction. The absence of the wild-type band in recipients of ACAT1$^{-/-}$ cells indicates complete repopulation of the marrow with cells of donor origin. (**b** and **c**) Immunocytochemical analyses of the proximal aorta. Cryosections (5 μm) were treated according to our previously published method (46) and stained for ACAT1 using a rabbit antibody to recombinant human ACAT1 (31).

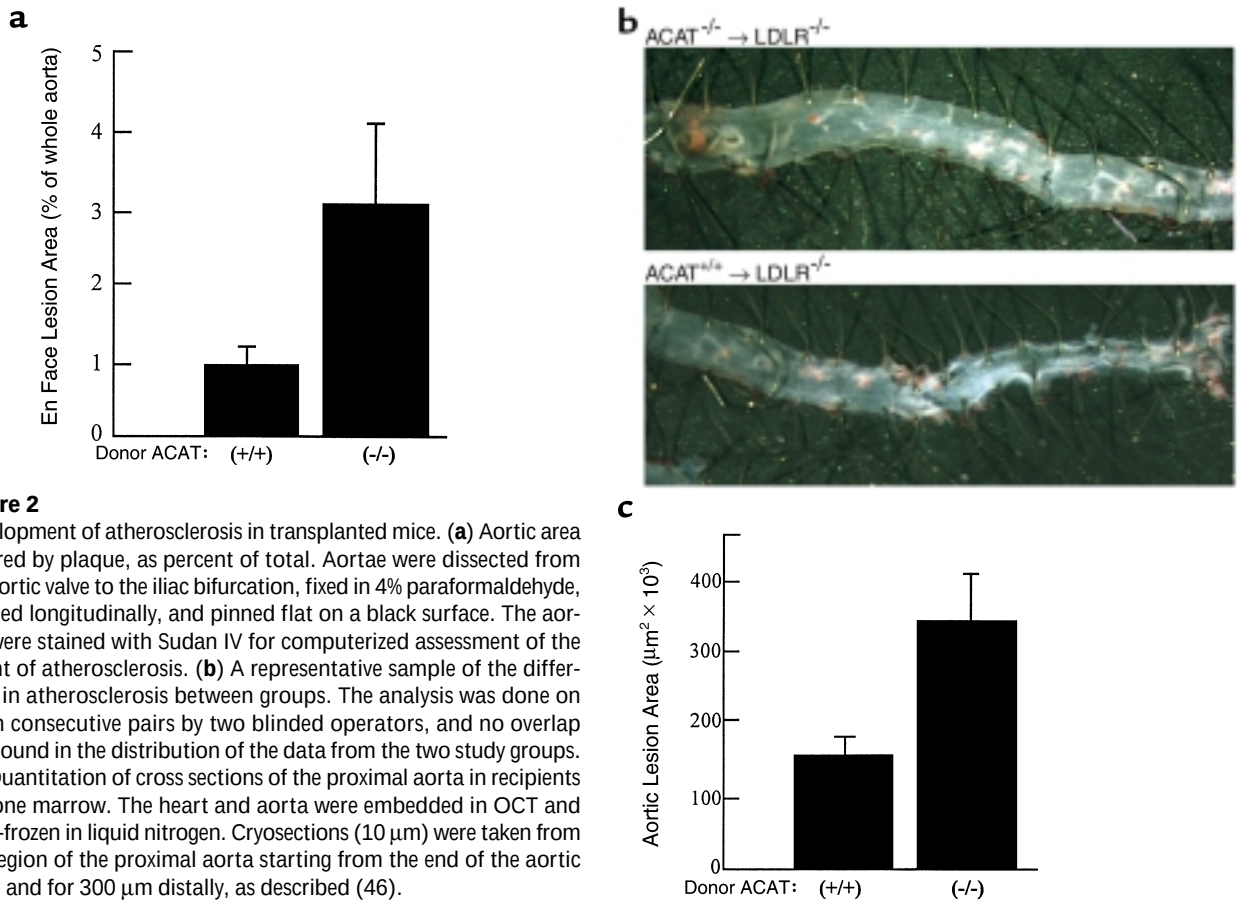

Figure 2
Development of atherosclerosis in transplanted mice. (**a**) Aortic area covered by plaque, as percent of total. Aortae were dissected from the aortic valve to the iliac bifurcation, fixed in 4% paraformaldehyde, opened longitudinally, and pinned flat on a black surface. The aortae were stained with Sudan IV for computerized assessment of the extent of atherosclerosis. (**b**) A representative sample of the difference in atherosclerosis between groups. The analysis was done on seven consecutive pairs by two blinded operators, and no overlap was found in the distribution of the data from the two study groups. (**c**) Quantitation of cross sections of the proximal aorta in recipients of bone marrow. The heart and aorta were embedded in OCT and snap-frozen in liquid nitrogen. Cryosections (10 μm) were taken from the region of the proximal aorta starting from the end of the aortic sinus and for 300 μm distally, as described (46).

Immunocytochemistry and Movat staining. Immunocytochemical staining of tissue samples for ACAT and macrophages was performed on 5-μm-thick serial cryosections from the proximal aortae. Sections were fixed in acetone and incubated with rabbit antibodies to recombinant human ACAT1 (31), the mouse monocyte-macrophage marker MOMA-2 (Accurate Chemical & Scientific Corp., Westbury, New York, USA), or, as smooth muscle cell marker, a rabbit affinity-purified antiserum to human smooth muscle myosin reacting with mouse myosin. The secondary antibodies were goat biotinylated antibodies to rabbit IgG (32). Primary antibodies were used at dilutions of 1:250, 1:300, and 1:30, respectively, and incubated overnight at 4°C. After washing, the sections were treated with goat biotinylated antibodies to rabbit and rat IgGs (both from PharMingen, San Diego, California, USA) and incubated with avidin-biotin complex labeled with alkaline phosphatase (Vector Laboratories, Burlingame, California, USA). The enzyme activity was visualized with Fast Red TR/Naphthol AS-NX substrate (Sigma Chemical Co.). Sections were counterstained with hematoxylin. Nonimmune rabbit and rat sera were used as negative controls in the place of primary antibodies. Photomicroscopy was performed on a Zeiss Axiophot with Plan-Neofluar objectives (Carl Zeiss Inc. Thornwood, New York, USA). To quantitate the area of the atherosclerotic lesions in the proximal aorta occupied by macrophages or smooth muscle cells, the area stained with MOMA-2 or actin in serial sections was measured using the Imaging System KS300 (Kontron Elektronik GmbH) as described above. The percentage of macrophages in the lesion was calculated as a ratio of the macrophage-stained area and the Oil-Red-O–stained area.

For Movat pentachrome staining, 5-μm aortic cryosections were fixed in 4% paraformaldehyde-PBS for 10 minutes and stained according to previously published methods (33, 34).

For terminal deoxynucleotidyl transferase–mediated dUTP nick end-labeling (TUNEL) staining, sections were permeabilized in 0.1% Triton X-100, 0.1% Na citrate. After incubation with deoxynucleotidyl transferase and fluorescein-labeled nucleotide mixture, sections were treated with alkaline phosphatase–conjugated anti-fluorescein antibody. Fast red TR/naphthol was used for color development. Controls for each experiment included serial sections treated with DNase (positive control) or incubated with the labeling solution without terminal transferase (negative control).

Results

Fetal liver cells or bone marrow from mice lacking ACAT1 (13) were transplanted into LDLR$^{-/-}$ mice (35), to generate mice with one of three ACAT1 genotypes: +/+, +/–, and –/–. Four weeks after transplantation, the mice were fed a western-type diet (containing 21% fat, 0.15% cholesterol, and no cholic acid) for 12 additional weeks. PCR analysis of bone marrow DNA extracted from recipient mice 8 weeks after transplantation showed a complete conversion of the ACAT genotype to the donor's type, indicating that the marrow population had been reconstituted (Figure 1a). Immunohistochemical studies of the artery wall confirmed the absence of ACAT1 immunoreactivity in mice transplanted with knockout cells compared with recipients of wild-type cells (Figure 1, b and c). As shown in Table 1, no differences were observed in plasma cholesterol and triglyceride levels between study groups, although a trend toward lower cholesterol levels was detected among recipients of ACAT1$^{-/-}$ macrophages ($P = 0.073$). Similarly, no differences were observed between groups in the distribution of cholesterol and triglycerides among the lipoproteins, including HDL (not shown).

Unexpectedly, the atherosclerotic lesion area in cross sections of the aortic root (μm^2/section/mouse ± SEM) was larger in recipients of ACAT1$^{-/-}$ marrow than in recipients of ACAT1$^{+/+}$ marrow ($2.3 \times 10^5 \pm 2.9 \times 10^4$ and $1.4 \times 10^5 \pm 1.4 \times 10^4$, respectively; $P = 0.007$). Lesion area in recipients of ACAT1$^{+/-}$ marrow was not different compared with recipients of control marrow, suggesting a lack of gene-dosage effect and no measurable consequences of a 50% reduction in cholesterol esterification in macrophages. Also, the area covered by plaque in pinned-out aortae (Figure 2a) was increased between two- and threefold in recipients of ACAT1$^{-/-}$ macrophages. Figure 2b shows a representative example of the increased aortic atherosclerosis in LDLR$^{-/-}$ mice that received ACAT1$^{-/-}$ marrow. The free cholesterol content in whole aortae was increased in ACAT1$^{-/-}$ marrow recipients (17.6 ± 1.6 vs. 11.5 ± 1.8 μg/mg protein in ACAT$^{+/+}$ recipients, $P = 0.013$), consistent with the lack of macrophage ACAT activity resulting in the accumulation of unesterified cholesterol. Importantly neutral lipids were detectable in the sinus and aortic lesions of recipients of ACAT1-null marrow, indicating the presence of cholesterol esters in the plaque. As described below, this effect can be due to the migration of ACAT1$^{+/+}$ smooth muscle cells from the media.

To confirm the atherosclerosis findings, a second experiment was performed in which male LDLR$^{-/-}$ mice were transplanted with bone marrow from LDLR$^{-/-}$ mice that were either wild-type or homozygous negative at the ACAT1 gene locus. Four weeks after transplantation, the mice were fed a butterfat diet (16% fat, 1.25% cholesterol, 0.5% cholic acid) for 10 weeks. As in the first experiment, there were no differences in plasma cholesterol levels among the study groups (Table 1), and significantly larger lesions were found in recipients of ACAT1$^{-/-}$ marrow than in recipients of ACAT1$^{+/+}$ marrow ($3.5 \times 10^5 \pm 7.4 \times 10^4$ and $1.6 \times 10^5 \pm 2.7 \times 10^4$ $P < 0.03$; Figure 2c).

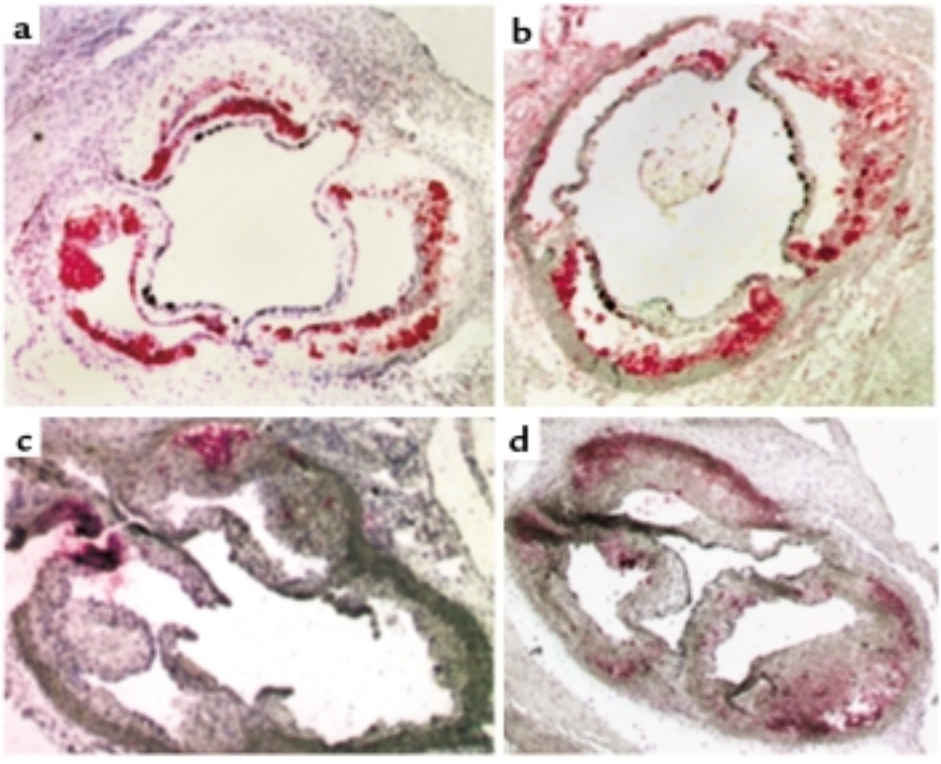

Figure 3
Immunocytochemical analyses of the proximal aorta in LDLR$^{-/-}$ mice after transplantation with ACAT1$^{+/+}$ (**a** and **c**) or ACAT1$^{-/-}$ cells (**b** and **d**). **a** and **b** show staining with MOMA 2 (a macrophage-specific marker). **c** and **d** show TUNEL staining. Sections were permeabilized in 0.1% Triton X-100, 0.1% Na citrate. After incubation with deoxynucleotidyl transferase and fluorescein-labeled nucleotide mixture, sections were treated with alkaline phosphatase–conjugated anti-fluorescein antibody. Fast Red TR/naphthol was used for color development. Controls for each experiment included serial sections treated with DNase (positive controls) or incubated with the labeling solution without terminal transferase (negative controls).

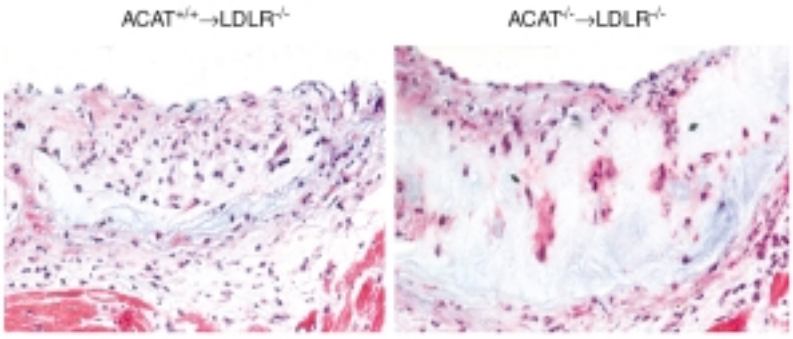

Figure 4
Movat's pentachrome staining of aortic cross sections from representative LDLR$^{-/-}$ mice after western-type diet. The left panel shows a representative section from a recipient of ACAT1$^{+/+}$ wild-type marrow, whereas the right panel shows a recipient of ACAT1$^{-/-}$ marrow. The lesion area in the control animal is highly cellular, and amorphous material is detected in the deeper portion of the plaque. This phenomenon is exaggerated in the ACAT1$^{-/-}$ recipient mouse, where lesions are thicker, less cellular, and more enriched in extracellular material than in controls. Nuclei are stained black, and smooth muscle cells are stained red. The blue stain indicates ground substance and mucins. The lack of yellow stain indicates the absence of significant collagen deposition. In each panel, the section is oriented with the lumen on top and the media at the bottom.

Immunohistochemical staining was performed on a subset of mice to analyze the effects of ACAT1 deficiency on lesion composition. Immunostaining for macrophages showed less staining in ACAT1$^{-/-}$ recipient mice (27.2% of the total lipid-stained area compared with 70.5% in recipients of ACAT1$^{+/+}$ marrow, a 61% difference; $P < 0.001$; $n = 10$ for ACAT1$^{+/+}$ recipients, and $n = 9$ for ACAT1$^{-/-}$ recipients). The sections shown in Figure 3, a and b, are not representative of the difference in lesion size between groups, but show the difference in macrophage staining distribution and the loss of macrophages in the deeper portions of the plaque in mice recipient of ACAT1$^{-/-}$ marrow (Figure 3a) compared with controls (Figure 3b).

Because in vitro studies have demonstrated that cholesterol toxicity associated with ACAT inhibition can cause cell death in macrophages (36–38), we examined the extent of apoptosis and necrosis in arterial lesions by TUNEL staining of aortic cross sections from study animals. The proportion of TUNEL-stained cells was threefold higher in ACAT1$^{-/-}$ recipient mice than in controls (18% vs. 52%, $P = 0.037$), indicating that necrotic and apoptotic cell death contributed to the diminished numbers of macrophages in lesions (Figure 3, c and d). The TUNEL-stained cells did not stain with antisera that recognizes either macrophage or smooth muscle cell antigens (not shown). However, we presume that the TUNEL-stained cells were macrophages because these cells were markedly reduced in the ACAT1$^{-/-}$ recipients and ACAT1 deficiency causes macrophage death in vitro (36–38).

In recipients of ACAT1$^{-/-}$ marrow, the areas of intense staining were concentrated in the deeper portions of the plaque, whereas viable macrophages were observed closer to the endothelial surface. This pattern suggests that macrophages that have recently migrated from the lumen are healthy and remain active until, with deeper migration and increasing residence time in the lesion, the cholesterol overload induces severe accumulation of unesterified cholesterol and promotes cell death. To determine whether the macrophage-poor lesions in recipients of ACAT$^{-/-}$ marrow had other unique morphologic and compositional features, additional evaluations of the remaining sections were done using the Movat's pentachrome stain and an anti-myosin antibody. Staining for smooth muscle cells was higher in recipients of ACAT1$^{-/-}$ marrow than in recipients of control marrow as absolute area (185,144 vs. 88,038 μm^2, respectively; $n = 5$ per group; $P = 0.05$), but it was no different than in controls when expressed as percentage of total lesion area. However, the lesion area occupied by acellular material was 37.6% in the ACAT1$^{-/-}$ recipient mice ($n = 6$) and 1.8% in the ACAT1$^{+/+}$ recipient controls ($P < 0.001$). Figure 4 shows a representative set of Movat's pentachrome stains, which demonstrate a large expansion of the core ground substance containing glycosaminoglycans and proteoglycans (blue stain) in ACAT1$^{-/-}$ recipients (Figure 4, right) relative to controls (Figure 4, left). Also, the picture shows the reduced cellularity of the lesion (nuclei are stained black), as well as the lack of elastic fibers (black) or collagen (yellow), and the relative increase in smooth muscle (red) in ACAT1$^{-/-}$ mice. Because proteoglycans are the secretory product of smooth muscle cells, the excess blue staining in aortic cross sections of ACAT$^{-/-}$ recipients is indicative of the preponderance of smooth muscle cells relative to macrophages in these lesions.

Discussion

This study addressed the question of whether the absence of macrophage ACAT1 in the setting of hyperlipidemia would reduce atherosclerosis. To test this, LDLR$^{-/-}$ mice of either gender underwent transplantation of marrow or fetal liver cells with or without the selective deletion of the ACAT1 gene, and were then exposed to high-fat diets that increased plasma cholesterol levels. Although no differences were observed in plasma lipids between groups, the lack of ACAT1 in macrophages unexpectedly produced increased lesion area in both the aortic root and the aorta. Plaques in recipients of ACAT1$^{-/-}$ marrow had reduced numbers of macrophages, probably as a consequence of increased macrophage death due to toxicity from unesterified cholesterol. The increase in

Table 1
Plasma lipid levels in transplanted mice

Fetal liver transplantation						
Time	$Acat1^{+/+}$ $n = 14$		$Acat1^{+/-}$ $n = 14$		$Acat1^{-/-}$ $n = 12$	
	Cholesterol	Triglycerides	Cholesterol	Triglycerides	Cholesterol	Triglycerides
Baseline	305 ± 77	84 ± 28	346 ± 110	118 ± 62	300 ± 124	122±78
4 weeks	259 ± 89	88 ± 23	265 ± 115	78 ± 19	316 ± 120	91 ± 24
8 weeks	654 ± 248	149 ± 51	572 ± 150	151 ± 59	532 ± 215	214 ± 155
12 weeks	618 ± 158	265 ± 164	595 ± 208	203 ± 73	590 ± 190	265 ± 136
16 weeks	677 ± 177	271 ± 99	635 ± 169	280 ± 124	522 ± 244	267 ± 178
Bone marrow transplantation						
Time	$Acat1^{+/+}$ $n = 6$		$Acat1^{-/-}$ $n = 6$			
	Cholesterol	Triglycerides	Cholesterol	Triglycerides		
Baseline	362 ± 39	167 ± 38	370 ± 33	135 ± 14		
4 weeks	420 ± 65	156 ± 26	436 ± 38	155 ± 45		
8 weeks	681 ± 193	420 ± 104	430 ± 169	257 ± 105		
12 weeks	1153 ± 172	139 ± 44	1141 ± 121	260 ± 121		
14 weeks	1043 ± 105	123 ± 26	953 ± 95	138 ± 57		

Serum cholesterol levels were determined using Sigma Kit no. 352 adapted for a microtiter plate assay, as previously described (27). Data are in mg/dl (mean ± SD).

lesion-free cholesterol due to macrophage ACAT1 deficiency probably acted as a proinflammatory stimulus, leading to increased lesion area. Immunostaining of lesion sections indicated that the increased lesion areas were attributable to increased content of smooth muscle cells and acellular material.

Our atherosclerosis results are in agreement with the increase in atherosclerosis found in transgenic mice overexpressing hormone-sensitive lipase (an intracellular cholesterol ester hydrolase that produces free cholesterol) in macrophages (39). Our findings also support the hypothesis that the accumulation of free cholesterol in the plaque results in macrophage death and fewer macrophages in the lesion. Similar qualitative decreases in macrophage content of lesions have been seen in atherosclerotic lesions in cholesterol-fed rabbits treated with ACAT inhibitors (10), as well as in $ACAT1^{-/-}$ mice crossed into $LDLR^{-/-}$ and $apoE^{-/-}$ backgrounds (22). In this latter study, the elimination of macrophage ACAT1 in hyperlipidemic mice resulted in untoward dermatologic effects characterized by massive xanthomatosis, deposition of cholesterol crystals, marked inflammatory response, and rupture of the subdermal muscle layer. In addition, the double knockout mice showed a significant reduction in plasma cholesterol levels, maybe because the skin was acting as a sink for plasma cholesterol deposition. Although this difference in cholesterol concentrations made it impossible to rigorously compare atherosclerotic lesion development in quantitative terms, it was evident that the hyperlipidemic mice lacking ACAT1 were not protected from the growth of arterial plaque (22). These data suggested that the lack of cholesterol esterification ability in the macrophage may not be antiatherogenic, and prompted us to conduct the present set of experiments to quantitatively analyze aortic atherosclerosis in hyperlipidemic mice who differ only for the presence or absence of macrophage ACAT1. Our findings of increased lesion areas in mice whose macrophages cannot produce esterified cholesterol suggest that an intervention that induces free cholesterol accumulation in the artery wall is followed by cell toxicity, cell death, and inflammation, and that these changes promote increased lesion area. We speculate that this result could be offset by interventions that would promote free cholesterol efflux. Although our results suggest that the paucity of macrophages in lesions is due to cell death, they do not exclude the possibility that macrophage influx into lesions is impaired in ACAT1 deficiency.

Our results differ somewhat from those recently reported by Yagyu et al. (40). These authors found that ACAT1 deficiency introduced into LDLR-null mice caused a moderate reduction in atherosclerosis without altering plasma cholesterol levels. However, the amount of atherosclerosis in ACAT1-deficient mice might have been underestimated in their study since neutral lipid staining was used to measure lesion size. Additionally, the apparent discrepancy might be due to differences in study design. In their study, there was a total ACAT1 deficiency in all cell types, whereas ACAT1 was selectively deficient in macrophages (and not in smooth muscle cells, for example) in our study.

Evidence that free cholesterol may be damaging to the artery wall comes from several observations. The cholesterol clefts typical of advanced lesions contain free cholesterol crystals, which may also serve as nucleation sites for calcification (41). Cholesterol crystals can also form intracellularly (42) and have been shown to induce macrophage cell toxicity and death (36–38), thus contributing to the expansion of the atheroma lipid core (43). It is likely that choles-

terol efflux through reverse cholesterol transport helps to protect macrophages from free cholesterol toxicity. However, in our study this protective mechanism may have been overwhelmed. In this regard, cholesterol efflux may be regulated less by the amount of intracellular free cholesterol than by the availability of extracellular cholesterol acceptors such as nascent HDL, apoAI, or apoE (44). Indeed, the addition of apoAI or apoE to the medium of J774 mouse macrophages incubated with the ACAT inhibitor CP113,818 reduced cholesterol crystal formation by 80%, indicating that both free cholesterol and acceptor molecules are required for the activation of cholesterol efflux (42).

Our results also differ from those of studies that used ACAT inhibitors in animals (7–10), in which reduced atherosclerosis was observed despite the lack of measurable effects of the compounds on plasma cholesterol. This apparent discrepancy may be due to effects of ACAT2 inhibition on the cholesterol ester content of lipoproteins, which may reduce the atherogenicity of the particle without affecting its plasma concentration. Because inhibitors lack specificity, a pharmacologic effect on ACAT2 would reduce the amount of esterified cholesterol inserted in the nascent VLDL, thus determining the production of particles that may have reduced atherogenicity. Also, ACAT1 inhibition induced by drugs is likely incomplete, so that a modest increase in free cholesterol may be countered by enhanced cholesterol efflux before it causes cell toxicity. In contrast, in our study, the complete absence of ACAT1 may have produced an overload of unesterified cholesterol in macrophages to levels that induced cell death.

In summary, our results show that ACAT1 deficiency in macrophages promotes rather than inhibits atherosclerotic lesion development. These data, together with the recent findings of massive xanthomatosis involving the skin and brain in severely hypercholesterolemic ACAT1$^{-/-}$ mice (22), suggest that selective and potent ACAT1 inhibition may not be a beneficial therapeutic strategy for treating or preventing atherosclerosis, and may in fact be detrimental. Although the reduced content of macrophages and neutral lipids in lesions lacking ACAT1 may have beneficial effects on lesion stability (10), the increase in lesion area and the possibility of previously unanticipated side effects (45) argue against selective inhibition of ACAT1 as a therapeutic strategy.

Acknowledgments

This work was supported in part by American Heart Association Grant-in-Aid 95011450 (to S. Fazio) and by NIH grants HL-53989 (to M.F. Linton), HL-57986 (to S. Fazio), and HL-57170 (R.V. Farese, Jr.). A.S. Major and M. Accad are recipients of NIH postdoctoral fellowships. S. Fazio and M.F. Linton are Established Investigators of the American Heart Association. We thank Ted Mazzone and Doug Vaughan for a critical reading of the manuscript, and Stephen Ordway for editorial assistance. We are indebted to Lily Liu and Nikki Joiner for technical assistance.

1. Yao, P.M., and Tabas, I. 2000. Free cholesterol loading of macrophages induces apoptosis involving the fas pathway. *J. Biol. Chem.* **275**:23807–23813.
2. Chang, T.Y., Chang, C.C.Y., and Cheng, D. 1997. Acyl-coenzyme A:cholesterol acyltransferase. *Annu. Rev. Biochem.* **66**:613–638.
3. Brown, M.S., and Goldstein, J.L. 1983. Lipoprotein metabolism in the macrophage: implications for cholesterol deposition in atherosclerosis. *Annu. Rev. Biochem.* **52**:223–261.
4. Krause, B.R., and Bocan, T.M.A. 1995. ACAT inhibitors: physiologic mechanisms for hypolipidemic and anti-atherosclerotic activities in experimental animals. In *Inflammation: mediators and pathways.* R.R. Ruffolo and M.A. Hollinger, editors. CRC Press. Boca Raton, Florida, USA. 173–198.
5. Sliskovic, D.R., and White, A.D. 1991. Therapeutic potential of ACAT inhibitors as lipid lowering and anti-atherosclerotic agents. *Trends Pharmacol. Sci.* **12**:194–199.
6. Matsuda, K. 1994. ACAT inhibitors as antiatherosclerotic agents. *Med. Res. Rev.* **14**:271–305.
7. Bocan, T.M.A., Mueller, S.B., Uhlendorf, P.D., Newton, R.S., and Krause, B.R. 1991. Comparison of CI-976, an ACAT inhibitor, and selected lipid-lowering agents for antiatherosclerotic activity in iliac, femoral, and thoracic/aortic lesions. A biochemical, morphological, and morphometric evaluation. *Arterioscler. Thromb.* **11**:1830–1843.
8. Matsuo, M., et al. 1995. Effect of FR145237, a novel ACAT inhibitor, on atherogenesis in cholesterol-fed and WHHL rabbits. Evidence for a direct effect on the arterial wall. *Biochim. Biophys. Acta.* **1259**:254–260.
9. Nicolosi, R.J., Wilson, T.A., and Krause, B.R. 1998. The ACAT inhibitor, CI-1011 is effective in the prevention and regression of aortic fatty streak in hamsters. *Atherosclerosis.* **137**:77–85.
10. Bocan, T.M., et al. 2000. The ACAT inhibitor avasimibe reduces macrophages and matrix metalloproteinase expression in atherosclerotic lesion of hypercholesterolemic rabbits. *Arterioscler. Thromb. Vasc. Biol.* **20**:70–79.
11. Chang, C.C.Y., Huh, H.Y., Cadigan, K.M., and Chang, T.Y. 1993. Molecular cloning and functional expression of human acyl-coenzyme A:cholesterol acyltransferase cDNA in mutant Chinese hamster ovary cells. *J. Biol. Chem.* **268**:20747–20755.
12. Uelmen, P.J., Oks, K., Sullivan, M., Chang, T.Y., and Chan, L. 1995. Tissue-specific expression and cholesterol regulation of acylcoenzyme A:cholesterol acyltransferase (ACAT) in mice. Molecular cloning of mouse ACAT cDNA, chromosomal localization, and regulation of ACAT in vivo and in vitro. *J. Biol. Chem.* **270**:26192–26201.
13. Meiner, V.L., et al. 1996. Disruption of the acyl-CoA:cholesterol acyltransferase gene in mice: evidence suggesting multiple cholesterol esterification enzymes in mammals. *Proc. Natl. Acad. Sci. USA.* **92**:14041–14046.
14. Meiner V., et al. 1997. Tissue expression studies on the mouse acyl-CoA:cholesterol acyltransferase gene (Acact): findings supporting the existence of multiple cholesterol esterification enzymes in mice. *J. Lipid Res.* **38**:1928–1933.
15. Miyazaki, A., et al. 1998. Expression of ACAT-1 protein in human atherosclerotic lesions and culture human monocytes-macrophages. *Arterioscler. Thromb. Vasc. Biol.* **18**:1568–1574.
16. Cases, S., et al. 1998. ACAT-2, a second mammalian acyl-CoA:cholesterol acyltransferase. *J. Biol. Chem.* **273**:26755–26764.
17. Anderson, R.A., et al. 1998. Identification of a form of acyl-CoA:cholesterol acyltranferase specific to liver and intestine in nonhuman primates. *J. Biol. Chem.* **273**:26747–26754.
18. Oelkers, P., Behari, A., Cromley, D., Bilheimer, J.T., and Sturley, S.L. 1998. Characterization of two human genes encoding acyl coenzyme A:cholesterol acyltranferase related enzymes. *J. Biol. Chem.* **273**:26765–26771.
19. Chang, C.C.Y., et al. 2000. Immunological quantitation and localization of ACAT-1 and ACAT-2 in human liver and small intestine. *J. Biol. Chem.* **275**:28083–28092.
20. Zhang, S.H., Reddick, R.L., Piedrahita, J.A., and Maeda, N. 1992. Spontaneous hypercholesterolemia and arterial lesions in mice lacking apolipoprotein E. *Science.* **258**:468–471.
21. Ishibashi, S., et al. 1993. Hypercholesterolemia in low density lipoprotein receptor knockout mice and its reversal by adenovirus-mediated gene delivery. *J. Clin. Invest.* **92**:883–893.
22. Accad, M., et al. 2000. Massive xanthomatosis and altered composition of atherosclerotic lesions in hyperlipidemic mice lacking ACAT1. *J. Clin. Invest.* **105**:711–719.
23. Tocci, A., Rezzoug, F., Aitouche, A., and Touraine, J.-L. 1994. Comparison of fresh, cryopreserved and cultured haematopoietic stem cells from fetal liver. *Bone Marrow Transplant.* **13**:641–648.

24. Babaev, V.R., et al. 1999. Macrophage lipoprotein lipase promotes foam cell formation and atherosclerosis in vivo. *J. Clin. Invest.* **103**:1697–1705.
25. Dreesen, J.C., Dumoulin, J.C., Evers, J.L., Geraedts, J.P., and Pieters, M.H. 1995. Multiplex polymerase chain reaction for sex determination of single mouse blastomers. *Hum. Reprod.* **10**:743–748.
26. Linton, M.F., Atkinson, J.B., and Fazio S. 1995. Prevention of atherosclerosis in apoE deficient mice by bone marrow transplantation. *Science.* **267**:1034–1037.
27. Fazio, S., Lee, Y.-L., Ji, Z.-S., and Rall, S.C., Jr. 1993. Type III hyperlipoproteinemic phenotype in transgenic mice expressing dysfunctional apolipoprotein E. *J. Clin. Invest.* **92**:1497–1503.
28. Paigen, B., Morrow, A., Holmes, P.A., Mitchell, D., and Williams, R.A. 1987. Quantitative assessment of atherosclerotic lesions in mice. *Atherosclerosis.* **68**:231–240.
29. Tangirala, R.K., Rubin, E.M., and Palinski, W. 1995. Quantitation of atherosclerosis in murine models: correlation between lesions in the aortic origin and in the entire aorta, and differences in the extent of lesions between sexes in LDL receptor-deficient and apolipoprotein E-deficient mice. *J. Lipid Res.* **36**:2320–2328.
30. Rudel, L.L., Kelley, K., Sawyer, J.K., Shah, R., and Wilson, M.D. 1998. Dietary monounsaturated fatty acids promote aortic atherosclerosis in LDL receptor-null, human apoB100-overexpressing transgenic mice. *Arterioscler. Thromb. Vasc. Biol.* **18**:1818–1827.
31. Chang, C.C.Y., et al. 1995. Regulation and immunolocalization of acylcoenzyme A:cholesterol acyltransferase in mammalian cells as studied with specific antibodies. *J. Biol. Chem.* **270**:29532–29540.
32. Babaev, V.R., et al. 1988. Identification of intimal subendothelial cells from human aorta in primary culture. *Atherosclerosis.* **71**:45–56.
33. Movat, H.Z. 1955. Demonstration of all connective tissue elements in a single section. *Arch. Pathol.* **60**:289.
34. Russell, K. 1972. Pentachrome stain modification. *Arch. Pathol.* **94**:187.
35. Ishibashi, S., Goldstein, J.L., Brown, M.S., Herz, J., and Burns, D.K. 1994. Massive xanthomatosis and atherosclerosis in cholesterol-fed low density lipoprotein receptor-negative mice. *J. Clin. Invest.* **93**:1885–1893.
36. Warner, G.J., Stoudt, G., Bamberger, M., Johnson, W.J., and Rothblat, G.H. 1995. Cell toxicity induced by inhibition of acyl coenzyme A:cholesterol acyltransferase and accumulation of unesterified cholesterol. *J. Biol. Chem.* **270**:5772–5778.
37. Kellner-Weibel, G., et al. 1998. Effects of intracellular free cholesterol accumulation on macrophage viability. A model for foam cell death. *Arterioscler. Thromb. Vasc. Biol.* **18**:423–431.
38. Maccarrone, M., Bellincampi, L., Melino, G., and Finazzi Agro, A. 1998. Cholesterol, but not its esters, triggers programmed cell death in human erythroleukemia K562 cells. *Eur. J. Biochem.* **253**:107–113.
39. Escary, J.-L., et al. 1999. Paradoxical effect on atherosclerosis of hormone-sensitive lipase overexpression in macrophages. *J. Lipid Res.* **40**:397–404.
40. Yagyu, H., et al. 2000. Absence of ACAT-1 attenuates atherosclerosis but causes dry eye and cutaneous xanthomatosis in mice with congenital hyperlipidemia. *J. Biol. Chem.* **275**:21324–21330.
41. Craven, B.M. 1976. Crystal structure of cholesterol monohydrate. *Nature.* **260**:727–729.
42. Kellner-Weibel, G., et al. 1999. Crystallization of free cholesterol in model macrophage foam cells. *Arterioscler. Thromb. Vasc. Biol.* **19**:1891–1898.
43. Ball, R.Y., et al. 1995. Evidence that the death of macrophage foam cells contributes to the lipid core of atheroma. *Atherosclerosis.* **114**:45–54.
44. Rothblat, G.H., et al. 1999. Cell cholesterol efflux: integration of old and new observations provides new insights. *J. Lipid Res.* **40**:781–796.
45. Brewer, H.B. 2000. The lipid-laden foam cell: an elusive target for therapeutic intervention. *J. Clin. Invest.* **105**:703–705.
46. Fazio, S., et al. 1997. Increased atherosclerosis in C57BL/6 mice reconstituted with apolipoprotein E null macrophages. *Proc. Natl. Acad. Sci. USA.* **94**:4647–4652.